Inhibition of Human Corneal Myofibroblast Formation

Xiaoqing Guo, Sriniwas Sriram, Jennifer A. Tran, Audrey E. K. Hutcheon, and James D. Zieske

Schepens Eye Research Institute/Massachusetts Eye and Ear and Department of Ophthalmology, Harvard Medical School, Boston, Massachusetts, United States

Correspondence: Xiaoqing Guo, Schepens Eye Research Institute/Massachusetts Eye and Ear and Department of Ophthalmology, Harvard Medical School, Boston, MA 02114, USA;
Xiaoqing_Guo@meei.harvard.edu.

Submitted: March 2, 2018
Accepted: June 2, 2018

Citation: Guo X, Sriram S, Tran JA, Hutcheon AEK, Zieske JD. Inhibition of human corneal myofibroblast formation. *Invest Ophthalmol Vis Sci*. 2018;59:3511–3520. https://doi.org/10.1167/iovs.18-24239

Purpose. Transforming growth factor-beta (TGF-β) isoform 1 (T1) is involved in corneal fibrotic wound healing by stimulating myofibroblast transformation and altering fibrotic gene expression. In this study, two specific inhibitors were used to dissect the relationship between myofibroblast generation and the TGF-β/Smad- or TGF-β/p38-signaling pathway in human corneal fibroblasts (HCF).

Methods. In HCF, Trx-SARA (Smad-pathway inhibitor) was used to block the TGF-β/Smad-signaling pathway, and the p38 inhibitor (p38inh, SB202190) was used to inhibit $p38^{MAPK}$, thus blocking the TGF-β/p38-signaling pathway. HCF ± Trx-SARA or Trx-GA (SARA control) were serum starved overnight in Eagle's minimum essential medium (EMEM) ± p38inh, grown in EMEM ± T1 ± p38inh for 24 hours, and then processed for indirect-immunofluorescence, Western blot, or quantitative real-time polymerase chain reaction to examine α-smooth muscle actin (αSMA) and other fibrotic genes, such as fibronectin, thrombospondin1, and type III collagen. In addition, the morphology and the effect of p38inh on myofibroblast phenotype after myofibroblast formation were examined.

Results. We observed that Trx-SARA had little effect on αSMA expression, indicating that blocking the Smad pathway did not significantly inhibit myofibroblast formation. However, p38inh did significantly inhibit αSMA and other fibrotic genes, thus efficiently preventing the transition of HCFs to myofibroblasts. In addition, morphology changed and αSMA decreased in myofibroblasts exposed to p38inh medium, as compared with controls.

Conclusions. HCF transition to myofibroblasts was mainly through the p38 pathway. Therefore, blocking the p38 pathway may be a potential therapeutic tool for human corneal fibrosis prevention/treatment, because it controls myofibroblast formation in human corneal cells, while leaving other functions of T1 unaffected.

Keywords: fibrosis, myofibroblasts, corneal fibroblasts, TGF-beta signaling pathway, p38 pathway

Corneal fibrosis is basically the wound-healing response of the cornea to different types of injuries, which fails to properly repair and preserve corneal structure. Corneal wounds, which result from trauma or refractive surgery, trigger a complex healing process that involves inflammation, activation of cell-signaling events, generation and release of numerous cytokines, apoptosis, proliferation, migration, adhesion, differentiation, and remodeling of the extracellular matrix (ECM).[1–9] Some of the obvious changes in the corneal stroma during this process are as follows: (1) keratocyte death in the wound area; (2) quiescent keratocyte activation to fibroblasts in the area adjacent to the wound site; (3) proliferation of fibroblasts and replenishment of the wound bed to remodel the wounded ECM; and (4) fibroblast, or other cell type, transformation to myofibroblasts,[4,8,10–15] which are a contractile stromal cell phenotype often identified by the presence of α-smooth muscle actin (αSMA) fibrils contained within the cell.[16] The formation of myofibroblasts and the increased deposition of fibrotic proteins in the ECM, allow for the cornea to rapidly repair the wound gap[17]; however, this wound-healing process results in a less than optimal tissue, namely an opaque cornea that interferes with vision that may even cause blindness.[18] The current solution to restore vision for most of these eyes is through corneal transplant surgery, which replaces the dysfunctional cornea with a healthy donor cornea.[19] However, the global shortage of transplant-grade donor corneal tissue greatly restricts the number of corneal transplantations performed. Therefore, there is enormous clinical benefit to studying, understanding the mechanisms involved, and finding ways to prevent scar formation in corneal wound healing. One method of preventing fibrosis may be by controlling the key step(s) in wound healing, such as blocking the transforming growth factor-beta (TGF-β)-signaling pathway with the p38 inhibitor (p38inh), a highly selective, potent, and cell-permeable compound that inhibits p38 MAP kinase ($p38^{MAPK}$). If successful, this potentially would alleviate the increasing demand for transplantable corneal tissue and treat other corneal injuries, which in the United States alone are estimated to be over one million annually.[4]

Many different growth factors and cytokines, including, but not exclusive to, epidermal growth factor, fibroblast growth factor, interleukin, keratinocyte growth factor, hepatocyte growth factor, platelet-derived growth factor, TGF-β, and tumor necrosis factor alpha, are expressed by corneal cells and activated to regulate the wound-healing process.[4] Of these various growth factors, TGF-β1 (T1), one of three TGF-β isoforms, has a central role in severe fibrotic diseases.[17,20–25] T1 has been found to stimulate myofibroblast transformation in

Table 1. Three Additional p38 Inhibitors Tested

p38 Inhibitor	Conc.	IC50*	References
SB202190	10 μM	p38α = 280 nM p38β = 350 nM	Manufacturer's Data Sheet[33]
Birb796	10 μM	p38α = 38 nM p38β = 65 nM p38γ = 200 nM p38δ = 520 nM	Cicenas J, et al. 2017[34]
SB239063	20 μM	p38α = 44 nM	Barone FC, et al. 2001[35]
SB203580	5 μM	p38 α and β = 0.6 μM $p38^{MAPK}$ = 0.3–0.5 μM	Bain J, et al. 2007[36]

Conc., concentration.

* Inhibitory concentration, concentration of an inhibitor where the response is reduced by half.

vivo and in vitro, and by binding to its receptors on the cell surface, T1 triggers signaling, which leads to the activation of either a non-Smad-signaling pathway, such as $p38^{MAPK}$, $Ras^{(ErK/MAPK)}$, PP2A, RhoA, and JNK, or the better-known Smad-signaling pathway.[26] In our previous studies, we found that TGF-β signaling was involved in corneal wound repair in debridement, keratectomy, and penetrating wound models, and the type of wound or extent of injury affected which TGF-β-signaling pathway was stimulated.[9,27] In addition, we found that different T1-target proteins, even the same target protein in different human corneal cell types, were regulated through different pathways.[28] It is known that T1 is a multifunctional growth factor that has pronounced effects on cell growth, proliferation, adhesion, and migration in a variety of cell types, as well as ECM synthesis and degradation. Also, T1 exhibits both exacerbating and ameliorating features, depending on the phase of disease and site of action.[23] The aim of this study was to dissect the signaling response of fibrotic genes to T1 in human corneal stromal cells. By doing so, we hoped to find a way to prevent the stromal cell transition to myofibroblasts by blocking specific TGF-β-signaling pathway(s) in the human cornea, while leaving other functions of T1 unaffected.

Materials and Methods

Human Corneal Fibroblast Isolation

Human corneal fibroblasts (HCF) were isolated from human corneal stromas, as described previously.[29] All procedures/methods used in these studies adhered to the tenets of the Declaration of Helsinki. Human corneas were obtained from the National Disease Research Interchange (Philadelphia, PA, USA). The study's experimental protocols were judged to be exempt from review by the Institutional Human Studies Committees at the Schepens Eye Research Institute/Massachusetts Eye and Ear. Briefly, human corneal stromal explants from donor eyes were placed in 6-well plates in regular medium (RM; Eagle's minimum essential medium [EMEM; ATCC, Manassas, VA, USA] plus 10% fetal bovine serum [Atlanta Biologicals, Flowery Branch, GA, USA]), and incubated at 37°C with 5% CO_2 until sufficient amounts of HCF migrated from the explants.

Production of HCF Cell Lines

We produced two cell lines (Trx-SARA-HCF and Trx-GA-HCF) by infecting HCF with a retrovirus containing either a Trx-SARA or Trx-GA plasmid, as described previously.[28] Trx-SARA is comprised of the rigid scaffold Trx (the *Escherichia coli* thioredoxin A protein) followed by the Smad-binding domain of SARA, which is a constrained 56-amino acid Smad-binding motif from the SARA (Smad anchor for receptor activation) protein. Trx-SARA blocks the Smad-signaling pathway by binding to the monomeric Smad proteins, thus reducing the level of Smad2 and 3 in complex with Smad4 after TGF-β stimulation. Trx-GA is a control Trx aptamer of Trx-SARA, which contains an 11-amino acid repeat of Gly-Ala.

Cell Culture

HCF ± Trx-SARA or Trx-GA were seeded in 100-mm dishes or chamber slides in RM until they reached 60% to 70% confluency, at which time, the cells were cultured either in basic medium (BM; EMEM only) to serum starve the cells overnight or in p38inh (SB202190; Sigma-Aldrich Corp., St. Louis, MO, USA) medium (BM + 10 μM p38inh) to serum starve and pretreat the cells with p38inh overnight. The concentration of p38inh SB202190 was determined based on published reports.[30–33] The next day, cells were treated in BM ± 2 ng/mL T1 (R&D Systems, Inc., Minneapolis, MN, USA) ± 10 μM p38inh for 24 hours. Cells were examined and brightfield images were obtained (Carl Zeiss Microscopy, LLC, Thornwood, NY, USA). Then, they were either harvested by trypsinization for Western blot (WB) or quantitative real-time polymerase chain reaction (qRT-PCR) or fixed in cold methanol for indirect immunofluorescence (IF). Experiments were performed in at least triplicate for each condition. To confirm the specificity of p38inh (SB202190), three additional p38inhs (Table 1) were randomly selected and tested in the same manner. All p38inhs were found to have similar results.

In addition, HCFs were cultured in RM until they were 70% confluent, at which time they were stimulated to become myofibroblasts by exposing them to RM ± 2 ng/mL T1 for 3 days. The T1 cells were then rinsed with PBS three times, split into four groups, and cultured in the following for 1, 2, 3, or 4 days (D1, D2, D3, or D4, respectively): (1) RM, (2) RM + 10 μM p38inh, (3) RM + 2 ng/mL T1, and (4) RM + 2 ng/mL T1 + 10 μM p38inh. Media was changed every day and any media that included T1 had freshly prepared T1 added every day to ensure similar T1 activity throughout the experiment. Cells in different culture conditions were collected at each time point.

SDS-PAGE and WB Analysis

SDS-PAGE and WB analysis were performed as previously described.[37] In brief, protein from cells was extracted with radioimmunoprecipitation assay buffer (10 mM Tris, 150 nM NaCl, 1% deoxycholic acid, 1% Triton X-100, 0.1% SDS, 1 mM EDTA; Sigma-Aldrich Corp.) plus protease inhibitors (aprotinin, phenylmethylsulfonyl fluoride, and sodium orthovanadate; Sigma-Aldrich Corp.). Protein samples of equal volume and protein were loaded onto gradient gels (8%–16% Tris-glycine gels; Invitrogen, Carlsbad, CA, USA), transferred onto nitrocellulose membrane (Bio-Rad; Hercules, CA), and incubated with primary antibodies αSMA (Abcam, Cambridge, MA, USA), p38α, phospho (p)-p38 (Santa Cruz Biotechnology, Inc., Dallas, TX, USA), cellular fibronectin (cFN; Sigma-Aldrich Corp.), thrombospondin-1 (TSP1; Thermo Scientific, Waltham, MA, USA), or β-actin (Sigma-Aldrich Corp.). Protein bands were viewed on an infrared imaging system (Odyssey; Li-Cor, Lincoln, NE, USA) by detecting secondary antibodies conjugated with IRDye 680RD or 800CW (Li-Cor). β-actin was used as an internal control.

Indirect Immunofluorescence

Cells were fixed with methanol and processed for IF, as described previously.[38] In brief, cells were blocked (1% bovine

Table 2. qRT-PCR Primer List and Sequences

Gene	Forward Primer (5′-. . .-3′)	Reverse Primer (5′-. . .-3′′)
αSMA[41]	GGTGACGAAGCACAGAGCAA	CAGTTGGTGATGATGCCATGTT
Col III[42]	GGTGCTCGGGGTAATGACG	TCCAGGGAATCCGGCAGTT
*β-actin**	GGACTTCGAGCAAGAGATGG	AGCACTGTGTTGGCGTACAG

* VHPS-110 (Real Time Primers; Elkins Park, PA, USA).

serum albumin + 0.1% Triton X-100 [Sigma-Aldrich Corp.]), incubated overnight at 4°C with anti-αSMA (Dako North America, Carpinteria, CA, USA), and then incubated for 1 hour at room temperature with the appropriate secondary antibody conjugated to fluorescein (Jackson ImmunoResearch, West Grove, PA, USA). Samples were mounted with mounting media containing 4′,6-diamidino-2-phenylindole (Vectashield; Vector Labs, Burlingame, CA, USA), a nuclear counterstain, and observed and photographed (Nikon Eclipse E800 equipped with an Andor Clara E camera and Nikon NIS Elements for Basic Research; Micro Video Instruments, Avon, MA, USA). Negative controls, where the primary antibody was omitted, were run with all experiments.

Quantitative Real-Time Polymerase Chain Reaction

As previously described,[39] qRT-PCR was performed to quantify the fibrosis-related genes αSMA and type III collagen (Col III). In brief, total RNA was extracted from HCF (Trizol; Thermo Fisher Scientific, Waltham, MA, USA), purified (Qiagen RNeasy Mini isolation kit; Qiagen, Inc.; Valencia, CA, USA), and reverse transcribed to cDNA (High Capacity cDNA Reverse Transcription Kit; Applied Biosystems, Carlsbad, CA, USA). The qRT-PCR SYBR Green assay was performed with cDNA in master mix (KAPA SYBR Fast qPCR master mix; KAPA Biosystems, Wilmington, MA, USA) with primers for αSMA, Col III, and β-actin (Table 2; CCIB DNA Core Facility at Massachusetts General Hospital, Cambridge, MA, USA). Amplification was performed (Eppendorf multiplex 2 real time PCR machine; Eppendorf, Hauppauge, NY, USA) with the following thermal cycling conditions: 2 minutes at 50°C, 10 minutes at 95°C, 40 cycles of 15 seconds at 95°C, and 1 minute at 60°C. Relative mRNA levels of specific genes were reported as 2(−ΔΔCt).[40] β-actin was used as internal control.

Results

αSMA- and TGF-β-Signaling Pathways

In initial studies, we used a stable Trx-SARA-expressing HCF cell line, Trx-SARA-HCF, to examine the role of the Smad pathway on αSMA expression in HCF. As seen in Figure 1, little, if any, αSMA expression was detected in all three HCF samples (HCF, TRX-GA, and Trx-SARA) when cultured in BM only; however, with the addition of T1, αSMA expression increased significantly in all three samples (**$P < 0.01$). Interestingly, the existence of Trx-SARA had little, if any, effect on αSMA expression, indicating that blocking the Smad pathway did not significantly inhibit αSMA protein expression in HCF. This suggests that T1 does not stimulate corneal fibrosis through the Smad pathway, but by some other means.

We then examined the role that the TGF-β/p38-signaling pathway plays on the expression of αSMA in HCF. First, we needed to confirm that the p38inh SB202190 could block the p38 pathway. As seen in Figure 2, we confirmed by WB the inhibitive effect of SB202190 on the phosphorylation of p38 in HCF, and we calculated and graphed (Fig. 2) the ratio of phospho (p)-p38/p38 in HCF treated with the following: (1) BM, (2) BM + T1, and (3) BM + T1 + p38inh. Compared with BM samples (Fig. 2, inset lanes 1–3), the phosphorylation of

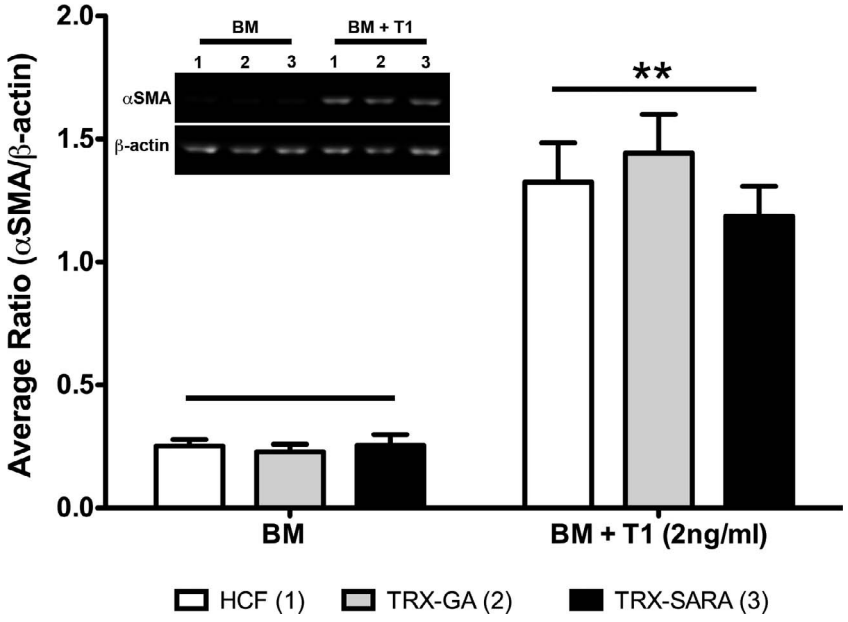

Figure 1. Analysis of TRX-SARA's effect on αSMA expression in HCF. HCF ± Trx-SARA or Trx-GA were either treated with EMEM (BM) or BM + 2 ng/mL of T1, and then examined for αSMA protein expression by WB. In all samples, αSMA protein expression increased significantly with T1 stimulation (**$P < 0.01$). Insert is a representative blot from three independent experiments. β-actin was used as the loading control.

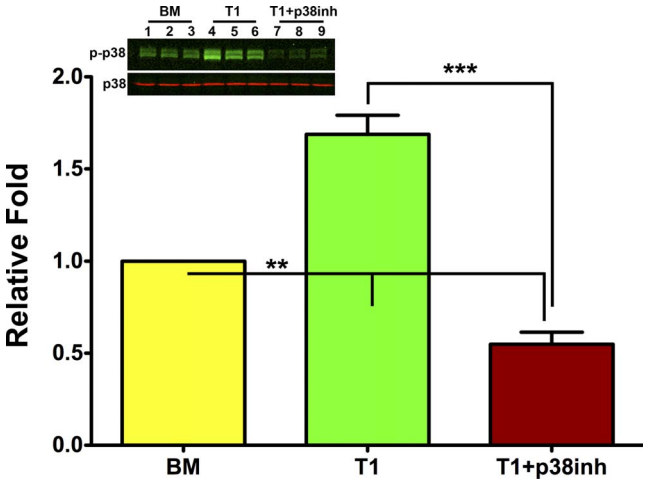

FIGURE 2. Confirmation by WB of the inhibitive effect of the p38 inhibitor SB202190 by examining phosphorylation of p38 in HCF. HCF were either treated with EMEM (BM), BM + T1 (2 ng/mL), or BM + T1 + p38inh (10 μM), and then examined for p38 and p-p38 protein expression by WB. The ratio of p-p38/p38 protein expression was graphed. Compared with BM samples (inset, lanes 1–3), the T1 samples (inset, lanes 4–6) were significantly upregulated and the T1 + p38inh samples (inset, lanes 7–9) were significantly downregulated (**$P < 0.01$). The addition of p38inh to T1-treated HCF efficiently inhibited the role of exogenous T1 on the phosphorylation of p38 (***$P < 0.001$).

p38 in the T1 samples (Fig. 2, inset lanes 4–6) was significantly upregulated (**$P < 0.01$). However, the addition of p38inh to HCF treated with T1 (Fig. 2, inset lanes 7–9), efficiently inhibited the role of exogenous T1 on the phosphorylation of p38 (***$P < 0.001$), and the p-p38 levels were significantly lower than the BM control (**$P < 0.01$). In addition, this p38inh, SB202190, effectively blocked the phosphorylation of the p38 protein by endogenous T1 to levels that were undetectable by WB (data not shown). These data indicate that p38inh effectively blocks the TGF-β/p38 pathway in HCF.

Since T1-treated HCF transition to myofibroblasts, we observed if p38inh altered the cellular morphology and αSMA localization in HCF by treating them as follows for 24 hours: (A) BM only, (B) BM + T1, (C) BM + p38inh, and (D) BM + T1 + p38inh. As seen in Figure 3, the cells appeared to be spindle shaped in both BM control (Fig. 3A) and BM + p38inh (Fig. 3C), similar to what would be expected for HCF. When T1 was added to BM (Fig. 3B), the cells changed from the fibroblastic spindle shape to a more myofibroblastic morphology, with stretched cellular hypertrophy and typical stress fibers.[43,44] Surprisingly, we found that the morphology of HCF in BM + T1 + p38inh (Fig. 3D) was similar to BM control and BM + p38inh (Figs. 3A, 3C). Therefore, the presence of p38inh in the T1 samples appeared to efficiently inhibit the morphologic transition of HCF to myofibroblasts by exogenous T1 (Fig. 3D).

The αSMA localization and protein expression shown in Figure 4 agrees with the morphologic data (Fig. 3). As with Figure 3, BM control and BM + p38inh had only a few αSMA-labeled cells (Fig. 4A.a, 4A.c) and little αSMA protein expression (Fig. 4B, lanes 1 and 3); however, with T1 treatment (Figs. 4A.b, 4B, lane 2), there were more αSMA-labeled cells and a significant increase in protein expression (***$P < 0.001$). By treating the HCF with BM + p38inh + T1 (Figs. 4A.d, 4B, lane 4), the number of αSMA-labeled cells appeared similar to controls (Figs. 4A.a, 4A.c), and the αSMA protein expression decreased significantly (***$P < 0.001$), as compared with BM + T1 samples (Fig. 4B, lane 2), returning to control levels (Fig. 4B, lanes 1 and 3), thus inhibiting the effect of exogenous T1 on the HCF. No staining was observed in negative controls (data not shown).

To test if p38inh offset the role of exogenous T1 in HCF at the transcription level, qRT-PCR was performed. As seen in Figure 5, αSMA mRNA levels in BM and BM + p38inh samples were lower than cells treated with BM + T1, which agrees with the morphologic and protein data shown in Figures 3 and 4. When HCF were treated with BM + T1 + p38inh, the effect of the exogenous T1 on the αSMA mRNA levels decreased significantly (*$P < 0.05$), indicating that by blocking the p38 pathway, αSMA mRNA expression was inhibited. These data indicate that regulation of αSMA expression by T1 in HCF is through the p38 pathway and when the p38 pathway is blocked, the transition of HCF to myofibroblasts is prevented.

To ensure the specificity of the p38inh SB202190, three other p38 inhibitors, Birb796, SB239063, and SB203580 (Table 1), were randomly selected and tested on HCF by using the same protocol as with SB202190. As seen in Figure 6, the results indicate that compared with HCF in BM + T1, the αSMA protein expression in HCF treated with these three other p38 inhibitors decreased in the presence of T1 (*$P < 0.05$). The concentrations of these three inhibitors were not optimized, and, therefore, if they were optimized, we believe the αSMA expression would be decreased to a greater and more significant extent. These data indicate that p38 signaling is very important for αSMA expression in HCF and that p38inh SB202190 is specific for the inhibition of p38 signaling.

Expression of Other Fibrosis-Related Genes and the p38 Pathway

The expression of certain fibrosis-related genes, such as cFN, TSP1, and Col III, has been shown to be upregulated in myofibroblasts at the mRNA and/or protein level.[37,45,46] In addition, TSP1 protein levels have been shown to significantly decrease when exposed to p38inh.[28] To examine if cFN and Col III were stimulated by T1 through the p38 pathway in HCF, HCF were cultured with BM ± T1 ± p38inh (SB202190) and examined by either WB or qRT-PCR. As with αSMA, cFN protein and Col III mRNA expression significantly increased in T1-treated HCF (Figs. 7A, 7B; *$P < 0.05$), as compared with control (BM only). When HCFs were treated with BM + T1 + p38inh, cFN protein (Fig. 7A, lane 4) and Col III mRNA expression (Fig. 7B) were greatly reduced, as compared with BM + T1 (*$P < 0.05$). In fact, cFN protein and Col III mRNA expression returned to control levels (BM only) or lower. Interestingly, unlike αSMA, cFN, and Col III, TSP1 did not return to control levels or lower, but rather only decreased by approximately one-third, indicating that another pathway may also be involved with activating TSP1.[28] These data indicate that cFN, TSP1, and Col III expression stimulated by T1 in HCF were at least partly regulated through the p38 pathway.

Role of p38 Inhibitor on Human Corneal Myofibroblast Phenotype

Since p38inh appeared to successfully inhibit myofibroblast formation due to T1 stimulation of HCF, we examined if the p38 inhibitor could not only reduce, but also reverse αSMA levels, thus changing the myofibroblast phenotype. As seen in Figure 8 (inset), the WB results showed that αSMA levels in T1-treated HCF (Fig. 8A, lane 2) were significantly higher than in the HCF control ($P < 0.001$; Fig. 8A, lane 1). On day 1 (D1), αSMA levels in both RM and p38inh groups continued to increase (Fig. 8A, lanes 3 and 4), compared with the T1-control (Fig. 8A, lane 2). On day 2 (D2), the αSMA levels in the RM sample leveled out (Fig. 8A, lane 5); however, in the p38inh sample (Fig. 8A, lane 6), the αSMA levels decreased and were

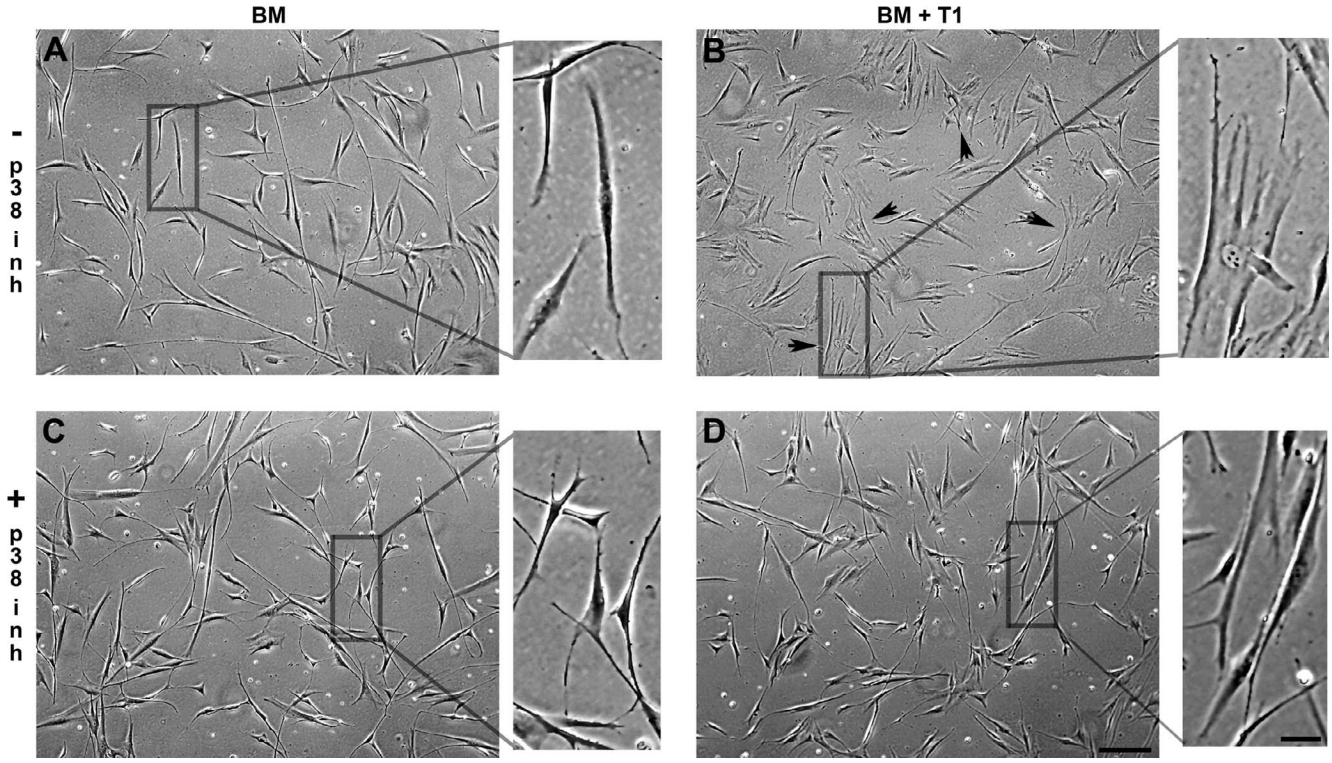

Figure 3. Morphologic comparison of HCF in different culture medium. A set of representative brightfield images of HCF cultured as follows: (**A**) BM (EMEM), (**B**) BM + T1 (2 ng/mL), (**C**) BM + p38inh (10 μM), and (**D**) BM + T1 + p38inh. With the addition of T1 (**B**), HCF appeared more myofibroblastic (*arrows* and excerpt); however, the presence of p38inh (**D**) efficiently inhibited the effect of exogenous T1 on HCF's transition to myofibroblast, thus causing the cells to appear more similar to controls (**A, C**). *Scale bars*: 200 μm (**D**) and 50 μm (**D**, excerpt).

significantly lower than the RM sample at D2 ($P < 0.05$). On day 3 (D3), αSMA levels in both media samples decreased (Fig. 8A, lane 7 and 8). Although both sample groups decreased, the αSMA level in the p38inh sample continued to be lower than that in the RM sample, which returned to T1 level.

As seen in Figure 8B, the mRNA data agreed with the protein data (Fig. 8A), in that T1-treated HCF mRNA expression was higher than the HCF control, and when the T1 samples were switched to RM only, the αSMA mRNA expression continued to increase at D1 and D2, appeared to peak at D2, and returned to almost T1 levels by D3. Interestingly, the αSMA mRNA expression of the samples that were switched to p38inh hovered around T1 levels at D1 and D2 and then decreased to control HCF αSMA mRNA levels by D3. These data indicate that although the human corneal myofibroblasts in RM returned to T1-control levels 3 days after the removal of T1 from the culture medium, the presence of the p38 inhibitor accelerated the change of the myofibroblast phenotype (Fig. 8B.D2).

In Figure 9, HCF samples where T1 was continuously present in the medium were observed. As seen in Figure 9A.a–k, the morphology of HCF cultured in RM only (Figs. 9A.c, 9A.f, 9A.i) for D1 to D4 remained relatively similar to HCF control (Fig. 9A.a); however, the T1-treated HCF became increasingly more myofibroblastic with time (Fig. 9A.d, 9A.g, 9A.j). By D4 with p38inh (Fig. 9A.k), the morphology of the HCF appeared to revert to that seen in the HCF control (Fig. 9A.a). Localization of αSMA was also examined at D4 (Fig. 9A.l–n) and the results agreed with the morphologic data (Fig. 9A.a–k). The D4 HCF control (Fig. 9A.l) had little to no αSMA localization, and T1 samples (Fig. 9A.m) had an increase in αSMA-positive cells. Interestingly, αSMA localization in T1 + p38inh samples (Fig. 9A.n) was similar to that of HCF controls (Fig. 9A.a). No staining was observed in negative controls (data not shown). These samples were also examined for αSMA protein levels (Fig. 9B), which increased when T1 was added to the medium. This increase continued to rise over time (T1-D3 compared with T1-control, $P < 0.001$); however, in samples with T1 + p38inh medium, αSMA levels increased on D1, decreased by D2, and significantly decreased by D3, as compared with T1-control ($P < 0.05$) and T1-D3 ($P < 0.01$). These data indicate that blocking the p38 pathway changed the phenotype of human corneal myofibroblasts.

Discussion

It is hard to completely avoid corneal injury, since injury can be caused by disease, accident, and even incisional surgery. Improper healing of these corneal wounds can lead to visual interference or even loss. In normal corneas, keratocytes are quiescent and structurally flattened cells found in the stroma; however, in wounded corneas, these cells are activated to become either fibroblasts or myofibroblasts, with the latter causing corneal fibrosis. T1, a key multifunctional growth factor that stimulates stromal cell transformation, is upregulated in corneal cells after a corneal wound and released into the stroma.[47,48] The T1 then binds to its receptors on the cell surface and produces a cascade effect via various intracellular signaling pathways, which activate the keratocytes to phenotypically change, ultimately transforming into myofibroblasts with high levels of αSMA. In addition to being associated with the development of stress fibers (αSMA) during corneal repair, T1 is also associated with cell proliferation and migration. Indeed, our previous studies have shown that HCF proliferation can be greatly inhibited by blocking the Smad pathway.[28] Therefore, to control the transition of HCF to myofibroblasts during wound repair while leaving the other functions of T1

Investigative Ophthalmology & Visual Science

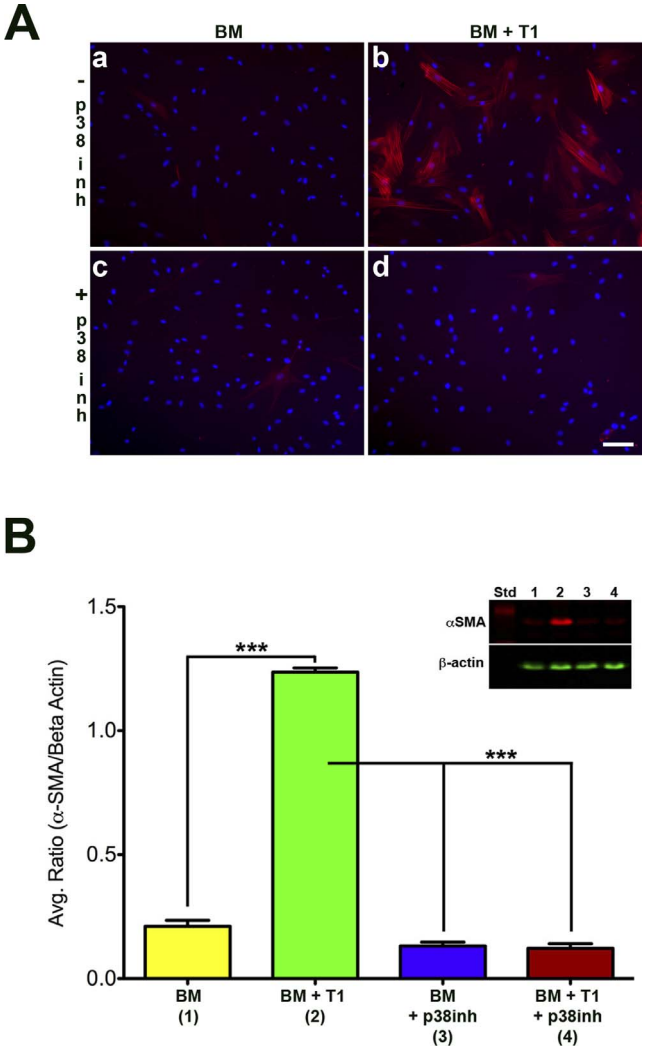

FIGURE 4. IF and WB analysis of the p38 inhibitor's effect on αSMA expression in HCF. (**A**) A set of representative IF images of HCF treated in the following medium: (**a**) BM, (**b**) BM + T1 (2 ng/mL), (**c**) BM + p38inh (10 μM), (**d**) BM + T1 + p38inh. Little, if any, αSMA localization was observed in controls: BM ± p38inh (**a**, **c**). As expected, αSMA localization increased with T1 stimulation (**b**); however, the presence of p38inh efficiently inhibited T1's role in αSMA protein expression (**d**). *Red*, αSMA; *Blue*, 4′,6-diamidino-2-phenylindole, a nuclear counterstain. *Scale bar*: 100 μm. (**B**) αSMA protein expression increased significantly in HCF with T1 stimulation (lane 2; $^{***}P < 0.001$), as compared with controls: BM ± p38inh (lanes 1 and 3); however, the addition of p38inh significantly inhibited T1's role on the αSMA protein levels (lane 4; $^{***}P < 0.001$), returning them back to control levels. Representative blot from one of three independent experiments is shown. β-actin was used as the loading control.

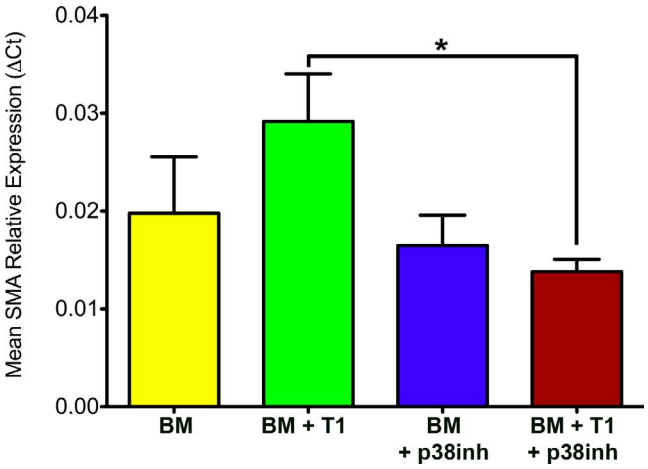

FIGURE 5. qRT-PCR analysis of p38 inhibitor's effect on αSMA expression in HCF. qRT-PCR was performed on HCF that were treated in the following medium: BM, BM + T1 (2 ng/mL), BM + p38inh (10 μM), and BM + T1 + p38inh. The relative mRNA expression of αSMA in each group was corrected with β-actin, an internal control. The role of exogenous T1 on αSMA mRNA expression in HCF was significantly prevented with the addition of p38inh ($^{*}P < 0.05$).

unaffected is extremely important and, we hope, would improve corneal healing results. To discern which pathway controls myofibroblast transition, two types of inhibitors were used in our studies to block either the TGF-β/Smad (Trx-SARA)- or TGF-β/p38 (p38inh, SB202190)-signaling pathways. After T1 stimulation, αSMA localization, as well as protein and mRNA expression, increased; however, no obvious change in αSMA expression, as compared with controls, was observed in HCFs containing Trx-SARA (Fig. 1), indicating that T1 did not affect the transition of HCFs to myofibroblasts through the Smad pathway. Surprisingly, when T1-stimulated HCFs were also treated with p38inh, not only did the morphology remain similar to controls (Fig. 3), but also the αSMA localization (Fig. 4A), protein expression (Fig. 4B), and mRNA expression (Fig. 5). This indicates that αSMA expression is regulated by T1 in HCF through the p38 pathway and by blocking the p38 pathway, the transition of HCF to myofibroblasts can be prevented, while leaving other T1 functions that occur through other signaling pathways (i.e., proliferation) unaffected.

The cornea is a transparent tissue, and the balance between ECM degradation and deposition in the stroma must be tightly regulated to maintain corneal function. Myofibroblasts are responsible for fibrotic-associated protein production, as well as ECM deposition and organization in wound healing.[37,45,46,49] If we are able to diminish this fibrotic-associated protein expression by preventing stromal cells in a

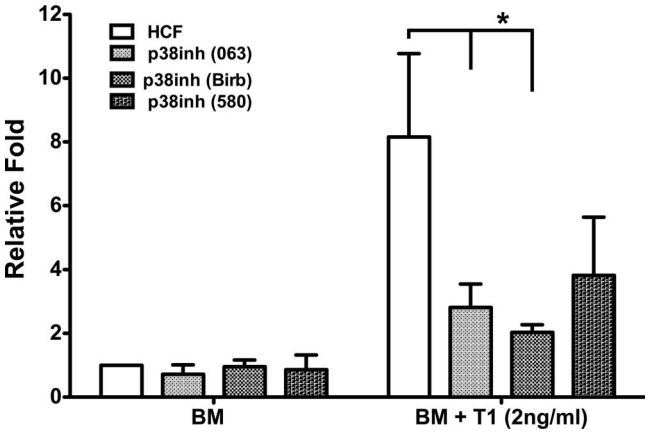

FIGURE 6. WB analysis of three additional p38 inhibitors' effect on HCF. The αSMA protein expression in HCF cultured with EMEM ± p38 inhibitor (p38inhs: 063 [SB239063]; Birb [Birb796], or 580 [SB203580]), or EMEM + 2 ng/mL T1 ± p38inh was analyzed. With the addition of T1 to samples, αSMA protein expression increased significantly ($^{***}P < 0.001$) in HCF controls; however, the p38 inhibitors decreased this expression in T1-stimulated cells. p38inhs (063 and Birb) decreased significantly ($^{*}P < 0.05$) as compared with HCF-T1 samples. β-actin was used as the loading control.

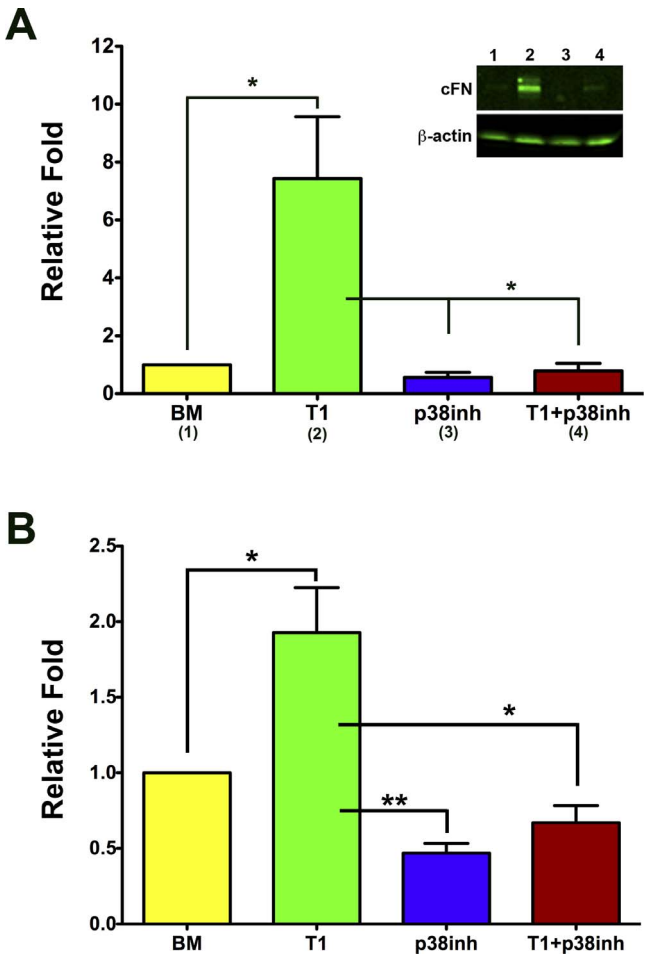

FIGURE 7. The role of the p38 inhibitor on cFN and Col III expression. HCF were cultured in the following medium: (1) BM, EMEM only, (2) T1, BM + T1 (2 ng/mL), (3) p38inh, BM + p38inh (10 μM), and (4) T1 + p38inh, BM + T1 + p38inh, and harvested for (**A**) WB analysis for cFN protein expression and (**B**) qRT-PCR analysis of Col III mRNA expression. (**A**) cFN protein expression increased significantly in T1-stimulated HCF (**A**, lane 2; $^*P < 0.05$) as compared with BM control. The addition of p38inh to T1 samples significantly inhibited T1's role on the cFN protein levels (**A**, lane 4; $^*P < 0.05$). A representative blot from one of three independent experiments is shown (inset). β-actin was used as the loading control. (**B**) Col III mRNA levels were upregulated by T1 ($^*P < 0.05$); however, the presence of p38inh efficiently inhibited T1's role in Col III mRNA expression ($^*P < 0.05$).

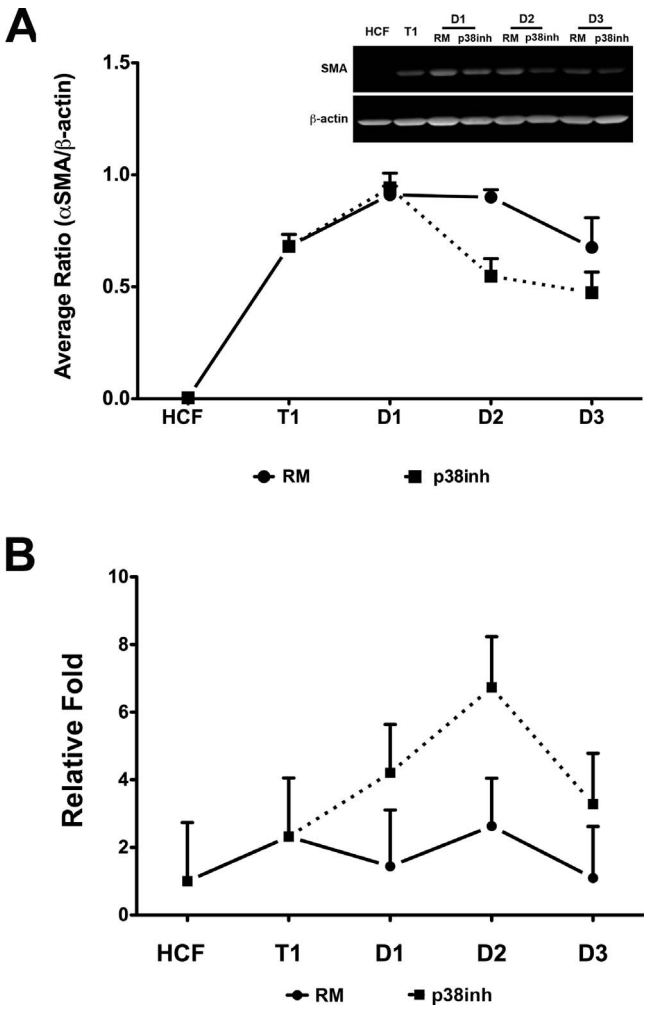

FIGURE 8. Analysis of αSMA expression in HCF cultured as follows: (1) HCF, RM (EMEM + 10% fetal bovine serum), (2) T1, RM + 2 ng/mL T1 (for 3 days), or (3) RM + T1 for 3 days, then RM ± p38inh for D1, D2, or D3. (**A**) Graph of αSMA WB corrected per lane with internal control (β-actin). αSMA expression in T1 samples was significantly different than in untreated cells (HCF; $P < 0.0001$). On D2, αSMA expression in p38inh-treated cells decreased significantly as compared with cells in RM ($P < 0.05$). (*Inset*) Representative WB image from one of three independent experiments. (**B**) Graph of relative αSMA mRNA corrected with β-actin, an internal control. αSMA mRNA data agree with protein data (**A**).

wounded cornea from transitioning to myofibroblasts, then we may be able to obtain scar-free healing. In the present study, with the addition of p38inh to T1-stimulated HCF, fibrotic protein or gene (cFN, TSP1, and Col III) expression was significantly reduced, similar to what was observed with αSMA, indicating that p38inh has the potential to decrease fibrotic protein deposition in ECM during corneal wound healing, and thus preventing the conversion of stromal cells to myofibroblasts

Fibrosis is defined as a persistent scar. In the cornea, when fibrosis occurs, the cornea becomes opaque, and, at present, the only treatment is transplantation. Interestingly, it has been reported that T1 expression increased in an animal model and patients with lung fibrosis,[9,25,50–52] indicating it is possible that T1 has a central role in persistent fibrosis. In addition, myofibroblasts have been found to persist in fibrotic organs and tissues, as well as to make fibrotic proteins.[17,48,53–56] Therefore, we hypothesized that blocking the p38 pathway would change the myofibroblasts back to fibroblasts, because p38inh has the ability to inhibit both exogenous and endogenous T1 in HCF (see Figs. 3–5). Our data indicate that with the addition of T1 to HCF in culture, αSMA protein expression increased, thus transitioning the HCF to myofibroblasts, and once the T1 was removed, p38inh enhanced the decrease in αSMA protein levels. When these myofibroblasts remained in T1 medium, the αSMA protein levels continued to increase with time, thus mimicking the fibrotic in vivo state (Fig. 9B). Excitingly, with the addition of p38inh to these cells, αSMA protein levels decreased similarly to those cells in p38inh-only medium (Fig. 8). These data were confirmed by morphology and localization studies (Fig. 9A, 9C), indicating that blocking the p38 pathway can change human corneal myofibroblast phenotypes in culture, which would be potentially important for the treatment of opaque corneas.

In conclusion, the results from this study indicate that HCF transition to myofibroblasts is mainly through the p38 pathway

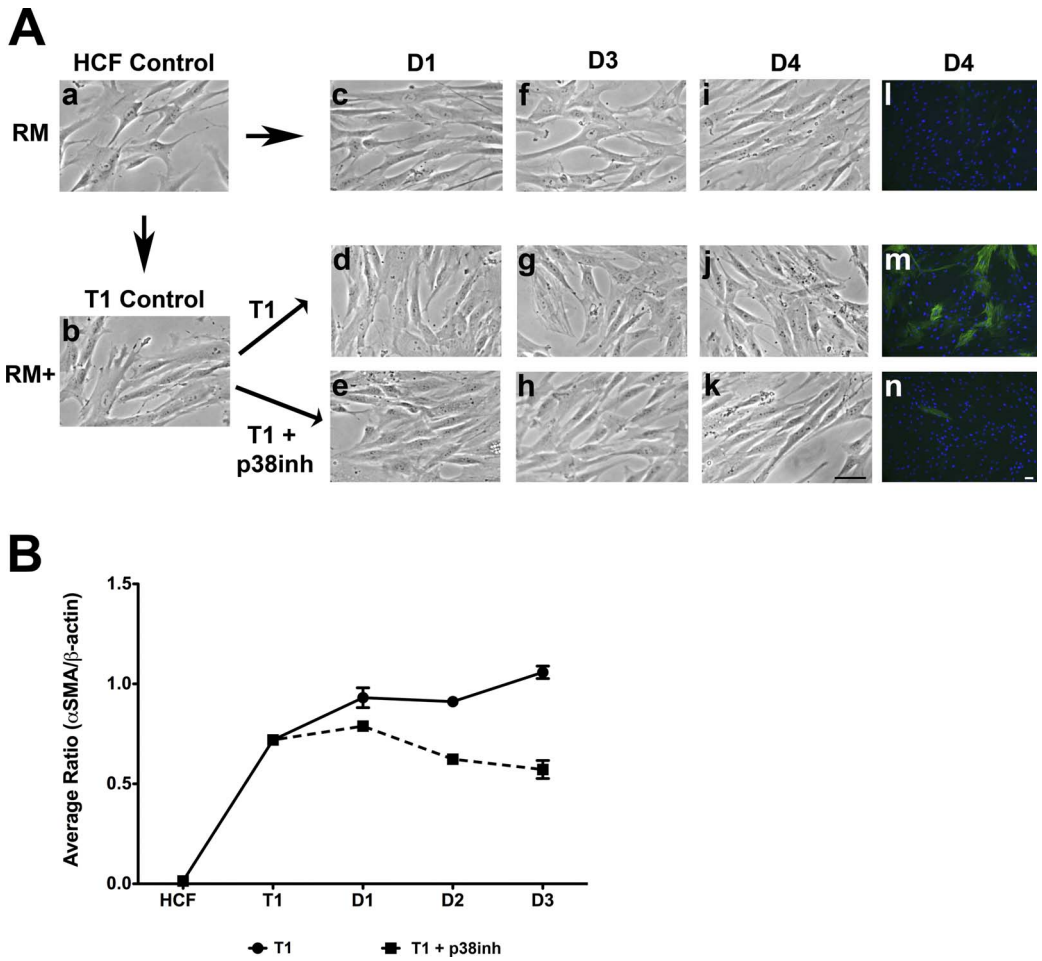

Figure 9. Effect of p38 inhibitor on T1-stimulated HCF in culture was analyzed by brightfield, IF, and WB. (**A**) Representative brightfield and IF images comparing HCF morphology (**a**–**k**) and αSMA localization (l–n) over time (D1, D2, D3, or D4) in media containing RM only (**c**, **f**, **i**, **l**), T1 (**d**, **g**, **j**, **m**), or T1+p38inh (**e**, **h**, **k**, **n**). The morphology of HCF cultured in RM only over 1 to 4 days (**c**, **f**, **i**) remained relatively similar to the HCF control (**a**); however, the T1-treated HCF became increasingly more myofibroblastic with time (**d**, **g**, **j**). Interestingly, the morphology of the HCF treated with both T1 and p38inh (**e**, **h**, **k**) became less myofibroblastic than the T1-control (**b**) and their T1-only counterparts (**d**, **g**, **j**). In addition, the morphology of the cells in D4 T1 + p38inh (**k**) appeared to revert to that seen in the HCF control (**a**), even though T1 was present in the media. *Scale bar*: 200 μm. The IF data (**l**–**n**) agreed with the morphologic data in D4 (**i**–**k**), with obvious αSMA in T1-treated HCF at D4 (**m**), and little, if any, αSMA in RM-only D4 (**l**) and T1+p38inh D4 (**n**). *Scale bar*: 50 μm. (**B**) Analysis of αSMA protein expression showed a significant increase in expression in T1 samples as compared with the HCF control ($P < 0.05$). This increase continued to rise over time (T1-D3 compared with T1-control, $P < 0.001$); however, in samples with T1 + p38inh medium, αSMA levels increased slightly on D1, decreased by D2, and significantly decreased by D3, as compared with T1-control ($P < 0.05$) and T1-D3 ($P < 0.01$).

and blocking the p38 pathway can reduce and reverse αSMA levels. In addition, other fibrotic-associated proteins were inhibited in T1-stimulated HCF. Therefore, the p38 inhibitor is a potential therapeutic tool for human corneal fibrosis prevention/treatment, because it controls myofibroblast formation in human corneal cells while leaving other functions of T1 unaffected.

Acknowledgments

The authors thank the National Disease Research Interchange for the use of tissues procured.

Supported by National Institutes of Health Grant 2 U42 OD011158 and National Institutes of Health/National Eye Institute Grants EY03790 (Core) and EY005665 (JDZ).

Disclosure: **X. Guo**, P; **S. Sriram**, None; **J.A. Tran**, None; **A.E.K. Hutcheon**, None; **J.D. Zieske**, P

References

1. Chen L, Mongan M, Meng Q, Wang Q, Kao W, Xia Y. Corneal wound healing requires IKB kinase beta signaling in keratocytes. *PLoS One*. 2016;11:e0151869.
2. Hutcheon AE, Guo XQ, Stepp MA, et al. Effect of wound type on Smad 2 and 4 translocation. *Invest Ophthalmol Vis Sci*. 2005;46:2362–2368.
3. Kato T, Nakayasu K, Kanai A. Corneal wound healing: immunohistological features of extracellular matrix following penetrating keratoplasty in rabbits. *Jpn J Ophthalmol*. 2000; 44:334–341.
4. Ljubimov AV, Saghizadeh M. Progress in corneal wound healing. *Prog Retin Eye Res*, 2015;49:17–45.
5. Riau AK, Angunawela RI, Chaurasia SS, Lee WS, Tan DT, Mehta JS. Early corneal wound healing and inflammatory responses after refractive lenticule extraction (ReLEx). *Invest Ophthalmol Vis Sci*. 2011;52:6213–6221.

6. Wilson SE, Mohan RR, Mohan RR, Ambrosio R Jr, Hong J, Lee J. The corneal wound healing response: cytokine-mediated interaction of the epithelium, stroma, and inflammatory cells. *Prog Retin Eye Res*. 2001;20:625–637.
7. Zieske JD. Expression of cyclin-dependent kinase inhibitors during corneal wound repair. *Prog Retin Eye Res*. 2000;19: 257–270.
8. Zieske JD, Guimaraes SR, Hutcheon AE. Kinetics of keratocyte proliferation in response to epithelial debridement. *Exp Eye Res*. 2001;72:33–39.
9. Zieske JD, Hutcheon AE, Guo X, Chung EH, Joyce NC. TGF-beta receptor types I and II are differentially expressed during corneal epithelial wound repair. *Invest Ophthalmol Vis Sci*. 2001;42:1465–1471.
10. Abdelkader A, Elewah E-SM, Kaufman HE. Confocal microscopy of corneal wound healing after deep lamellar keratoplasty in rabbits. *Arch Ophthalmol*. 2010;128:75–80.
11. Ashby BD, Garrett Q, Willcox MDP. Corneal injuries and wound healing—review of processes and therapies. *Austin J of Clin Ophthalmol*. 2014;1:1017.
12. Baum J, Duffy HS. Fibroblasts and myofibroblasts: what are we talking about? *J Cardiovasc Pharmacol*. 2011;57:376–379.
13. Campos M, Szerenyi K, Lee M, McDonnell JM, Lopez PF, McDonnell PJ. Keratocyte loss after corneal deepithelialization in primates and rabbits. *Arch Ophthalmol*. 1994;112: 254–260.
14. Myrna KE, Pot SA, Murphy CJ. Meet the corneal myofibroblast: the role of myofibroblast transformation in corneal wound healing and pathology. *Vet Ophthalmol*. 2009; 12(suppl 1):25–27.
15. Wilson SE, Chaurasia SS, Medeiros FW. Apoptosis in the initiation, modulation and termination of the corneal wound healing response. *Exp Eye Res*. 2007;85:305–311.
16. Hinz B, Celetta G, Tomasek JJ, Gabbiani G, Chaponnier C. Alpha-smooth muscle actin expression upregulates fibroblast contractile activity. *Mol Biol Cell*. 2001;12:2730–2741.
17. Bochaton-Piallat ML, Gabbiani G, Hinz B. The myofibroblast in wound healing and fibrosis: answered and unanswered questions. *F1000Res*. 2016;5:F1000 Faculty Rev-752.
18. Wilson SE. Corneal myofibroblast biology and pathobiology: generation, persistence, and transparency. *Exp Eye Res*. 2012; 99:78–88.
19. Amiri F, Ghiyasvandian S, Navab E, Zakerimoghadam M. Corneal transplantation: a new view of life. *Electron Physician*. 2017;9:4055–4063.
20. Moore BB, Lawson WE, Oury TD, Sisson TH, Raghavendran K, Hogaboam CM. Animal models of fibrotic lung disease. *Am J Respir Cell Mol Biol*. 2013;49:167–179.
21. Biernacka A, Dobaczewski M, Frangogiannis NG. TGF-beta signaling in fibrosis. *Growth Factors*. 2011;29:196–202.
22. Kenyon NJ, Ward RW, McGrew G, Last JA. TGF-beta1 causes airway fibrosis and increased collagen I and III mRNA in mice. *Thorax*. 2003;58:772–777.
23. Pohlers D, Brenmoehl J, Loffler I, et al. TGF-beta and fibrosis in different organs—molecular pathway imprints. *Biochim Biophys Acta*. 2009;1792:746–756.
24. Sanderson N, Factor V, Nagy P, et al. Hepatic expression of mature transforming growth factor beta 1 in transgenic mice results in multiple tissue lesions. *Proc Natl Acad Sci U S A*. 1995;92:2572–2576.
25. Molina-Molina M, Lario S, Luburich P, Ramirez J, Carrion MT, Xaubet A. Quantifying plasma levels of transforming growth factor beta1 in idiopathic pulmonary fibrosis [in Spanish]. *Arch Bronconeumol*. 2006;42:380–383.
26. Derynck R, Zhang YE. Smad-dependent and Smad-independent pathways in TGF-beta family signalling. *Nature*. 2003; 425:577–584.
27. Blanco-Mezquita JT, Hutcheon AE, Zieske JD. Role of thrombospondin-1 in repair of penetrating corneal wounds. *Invest Ophthalmol Vis Sci*. 2013;54:6262–6268.
28. Guo X, Hutcheon AEK, Tran JA, Zieske JD. TGF-beta-target genes are differentially regulated in corneal epithelial cells and fibroblasts. *New Front Ophthalmol*. 2017;3:10.15761/ NFO.1000151.
29. Guo X, Hutcheon AE, Melotti SA, Zieske JD, Trinkaus-Randall V, Ruberti JW. Morphologic characterization of organized extracellular matrix deposition by ascorbic acid-stimulated human corneal fibroblasts. *Invest Ophthalmol Vis Sci*. 2007; 48:4050–4060.
30. Menon MB, Dhamija S, Kotlyarov A, Gaestel M. The problem of pyridinyl imidazole class inhibitors of MAPK14/p38alpha and MAPK11/p38beta in autophagy research. *Autophagy*. 2015;11:1425–1427.
31. Parker LC, Luheshi GN, Rothwell NJ, Pinteaux E. IL-1 beta signalling in glial cells in wildtype and IL-1RI deficient mice. *Br J Pharmacol*. 2002;136:312–320.
32. Strittmatter F, Gratzke C, Walther S, et al. Alpha1-adrenoceptor signaling in the human prostate involves regulation of p38 mitogen-activated protein kinase. *Urology*. 2011;78:969.7–13.
33. Biomol GmbH. SAPK2, p38 MAPK Inhibitor (SB 202190) (Stressactivated Protein Kinase 2), Highly Purified | CAS 152121-30-7. Available at: https://www.biomol.com/product_ SAPK2-p38-MAPK-Inhibitor-SB-202190-Stress-activated-Protein-Kinase-2-Highly-Purified.html?aRelated=S0096-25.
34. Cicenas J, Zalyte E, Rimkus A, Dapkus D, Noreika R, Urbonavicius S. JNK, p38, ERK, and SGK1 inhibitors in cancer. *Cancers (Basel)*. 2017;10:1.
35. Barone FC, Irving EA, Ray AM, et al. Inhibition of p38 mitogen-activated protein kinase provides neuroprotection in cerebral focal ischemia. *Med Res Rev*. 2001;21:129–145.
36. Bain J, Plater L, Elliott M, et al. The selectivity of protein kinase inhibitors: a further update. *Biochem J*. 2007;408:297–315.
37. Guo X, Hutcheon AE, Zieske JD. Molecular insights on the effect of TGF-beta1/-beta3 in human corneal fibroblasts. *Exp Eye Res*. 2016;146:233–241.
38. Zieske JD, Mason VS, Wasson ME, et al. Basement membrane assembly and differentiation of cultured corneal cells: importance of culture environment and endothelial cell interaction. *Exp Cell Res*. 1994;214:621–633.
39. Sriram S, Tran JA, Guo X, Hutcheon AEK, Kazlauskas A, Zieske JD. Development of wound healing models to study TGFbeta3's effect on SMA. *Exp Eye Res*. 2017;161:52–60.
40. Livak KJ, Schmittgen TD. Analysis of relative gene expression data using real-time quantitative PCR and the 2−ΔΔCT method. *Methods*. 2001;25:402–408.
41. Zhou Q, Wang Y, Yang L, et al. Histone deacetylase inhibitors blocked activation and caused senescence of corneal stromal cells. *Mol Vis*. 2008;14:2556–2565.
42. Janin-Manificat H, Rovere MR, Galiacy SD, et al. Development of ex vivo organ culture models to mimic human corneal scarring. *Mol Vis*. 2012;18:2896–2908.
43. Hinz B. Formation and function of the myofibroblast during tissue repair. *J Invest Dermatol*. 2007;127:526–537.
44. Thannickal VJ, Lee DY, White ES, et al. Myofibroblast differentiation by transforming growth factor-beta1 is dependent on cell adhesion and integrin signaling via focal adhesion kinase. *J Biol Chem*. 2003;278:12384–12389.
45. Chen Y, Leask A, Abraham DJ, et al. Thrombospondin 1 is a key mediator of transforming growth factor beta-mediated cell contractility in systemic sclerosis via a mitogen-activated protein kinase kinase (MEK)/extracellular signal-regulated kinase (ERK)-dependent mechanism. *Fibrogenesis Tissue Repair*. 2011;4:9.
46. Xu H, Han X, Meng Y, et al. Favorable effect of myofibroblasts on collagen synthesis and osteocalcin production in the

Investigative Ophthalmology & Visual Science

periodontal ligament. *Am J Orthod Dentofacial Orthop*. 2014;145:469–479.

47. Tandon A, Tovey JC, Sharma A, Gupta R, Mohan RR. Role of transforming growth factor Beta in corneal function, biology and pathology. *Curr Mol Med*. 2010;10:565–578.
48. Torricelli AA, Santhanam A, Wu J, Singh V, Wilson SE. The corneal fibrosis response to epithelial-stromal injury. *Exp Eye Res*. 2016;142:110–118.
49. Jester JV, Petroll WM, Cavanagh HD. Corneal stromal wound healing in refractive surgery: the role of myofibroblasts. *Prog Retin Eye Res*. 1999;18:311–356.
50. Fernandez IE, Eickelberg O. The impact of TGF-beta on lung fibrosis: from targeting to biomarkers. *Proc Am Thorac Soc*. 2012;9:111–116.
51. Sumioka T, Kitano A, Flanders KC, et al. Impaired cornea wound healing in a tenascin C-deficient mouse model. *Lab Invest*. 2013;93:207–217.
52. Todd NW, Luzina IG, Atamas SP. Molecular and cellular mechanisms of pulmonary fibrosis. *Fibrogenesis Tissue Repair*. 2012;5:11.
53. Castellone MD, Laukkanen MO. TGF-beta1, WNT, and SHH signaling in tumor progression and in fibrotic diseases. *Front Biosci* (*Schol Ed*). 2017;9:31–45.
54. Hinz B, Phan SH, Thannickal VJ, et al. Recent developments in myofibroblast biology: paradigms for connective tissue remodeling. *Am J Pathol*. 2012;180:1340–1355.
55. Thannickal VJ. Mechanisms of pulmonary fibrosis: role of activated myofibroblasts and NADPH oxidase. *Fibrogenesis Tissue Repair*. 2012;5:S23.
56. Dawson D, Kramer T, Grossniklaus H, O Waring G, Edelhauser H. Histologic, ultrastructural, and immunofluorescent evaluation of human laser-assisted in situ keratomileusis corneal wounds. *Arch Ophthalmol*. 2005;123:741–756.